

THE SHAPE OF BI-DIRECTIONAL REFLECTION FROM NONHOMOGENEOUS OCEANIC BOUNDARY LAYER CLOUDS

Lin H. Chambers

*Atmospheric Sciences Division,
NASA Langley Research Center, Hampton, Virginia*

Received December 7, 1998

Accepted February 8, 1999

Theoretically generated bi-directional reflection functions for nonhomogeneous oceanic boundary clouds are studied using a singular value decomposition algorithm in an attempt to find simple parameterization as a function of cloud properties. Results suggest that this should be possible using 4–6 cloud properties; but those cloud properties tried to date have not satisfactorily reproduced the shape of the bi-directional function.

1. INTRODUCTION

Knowledge of the bi-directional reflection from the Earth's surface, including cloud cover when present, is required to accurately interpret measurements of radiance made by space-based instruments. For clouds, the reflection pattern expected based on the microphysical composition of the cloud can be radically altered by the cloud macrophysics; that is, by the cloud shape and internal inhomogeneities in cloud properties.

This paper studies the bi-directional reflection patterns of clouds at 0.83 μm visible wavelength using theoretical simulations, and attempts to develop a way to parameterize these patterns in terms of the properties of the cloud field. Sample cloud fields built from the horizontal pattern of cloudiness in 45 Landsat scenes of marine boundary layer cloud are used. These scenes include broken stratus and trade cumulus cases, as well as overcast scenes.^{1,2}

The current work has a number of limitations: 1) the independent pixel approximation (IPA) is used initially to derive the Landsat two-dimensional (2D) optical depth distributions which then generate the «true» cloud field; 2) only 2D (vertical and one horizontal dimension) cloud sections are treated so the full effects of 3D cloud field are not accounted for; 3) only single-layer low-level water clouds are considered; 4) conservative scattering (no absorption) is assumed; 5) a linear variation of cloud liquid water content with height in the cloud is assumed so there are no cloud holes.

Section 2 describes the generation of realistic inhomogeneous cloud fields from the Landsat scenes. Section 3 outlines the radiative transfer model and describes the parameters of interest in this study. Section 4 describes a singular value decomposition analysis of the bi-directional reflection patterns. Section 5 summarizes the major points and conclusion of this work.

2. GENERATION OF CLOUD SCENES

a. Landsat inferred horizontal inhomogeneity

Forty-five Landsat scenes of marine boundary layer cloud were available for use in this study.^{1,2} These were chosen from a total of 52 scenes by imposing a maximum of 10% of saturated pixels in each scene. The radiance field was converted to an optical depth field using 1D theory, with radiance thresholds determined by trial and error for each scene. A scene is about 58 km square, and consists of 2048 by 2048 pixels at 28.5 m spatial resolution (except for a few scenes of 1024 by 1024 pixels at a coarser resolution). To select 2D cloud scenes, 60 evenly placed 10 km long strips are distributed over each scene. The cloud fraction and mean cloud optical depth are computed for each strip. Samples are then selected from all scenes to fill as much as possible (20 samples were considered sufficient) a 6 by 6 matrix of cloud fraction and cloud optical depth (see Table I). This results in 341 sample cloud scenes. Note that not all bins are filled during this process: apparently marine boundary layer clouds do not occur in nature with optical depth > 20 and cloud fraction < 0.25, for example.

TABLE I. Cloud scene samples in cloud fraction (A_c) and mean cloud optical depth (τ).

τ	A_c					
	0–0.01	0.01–0.25	0.25–0.50	0.50–0.75	0.75–0.99	0.99–1
0–2.5	20	20	20	20	20	9
2.5–6	0	20	20	20	20	20
6–10	0	7	9	14	20	20
10–18	0	3	2	4	11	20
18–40	0	0	0	0	2	20
> 40	0	0	0	0	0	0

b. Modeled vertical inhomogeneity

The vertical dimension of the cloud field is generated based on an assumed linear variation of liquid water content with height within the cloud. This results in cloud water droplets whose size increases as the 1/3 power of their height within the cloud, while extinction increases as the 2/3 power of height. The shape of the clouds is imposed to match the statistics on cloud top bumpiness obtained from the Lidar In-Space Technology Experiment (LITE, Ref. 3). This requires placing 80% of the cloud above and 20% below some nominal level in the atmosphere. Resulting cloud top bumps vary in vertical size from a few meters to 200 m, with a typical size of 50–60 m.

The microphysical properties (extinction and particle size) are discretized onto a computational grid for input to the radiative transfer model. The input field also includes Rayleigh scattering effects in the atmosphere at the 0.83 μm wavelength for which the analysis is performed. The atmosphere is simulated above but not below the cloud. A black surface is assumed, to isolate the cloud effects.

3. TOOLS AND VARIABLES

a. Radiative transfer model

The radiation model used in this study is the Spherical Harmonics Discrete Ordinates Method.⁴ In brief, it uses both spherical harmonics and discrete ordinates to represent the radiance field during different segments of the solution algorithm. The spherical harmonics are employed for efficiently computing the source function including the scattering integral. The discrete ordinates are used to integrate the radiative transfer equation through the spatial grid. The solution method is to simply iterate between the source function and radiance field, and is akin to a successive order of scattering approach.

For each sample, 2D radiative transfer solutions are obtained for 10 solar zenith angles, θ_0 : 0°, 5°, then every 10° to 85°. Results obtained are the flux at the top of the cloud as a function of x , and the radiance at the cloud top as a function of x for 109 viewing angles (view zenith $\theta = 0^\circ$; and all combinations of $\theta = 5^\circ, 15^\circ, 25^\circ, 35^\circ, 45^\circ, 55^\circ, 65^\circ, 75^\circ, 85^\circ$, and relative azimuth $\phi = 0^\circ, 5^\circ, 20^\circ, 40^\circ, 60^\circ, 80^\circ, 100^\circ, 120^\circ, 140^\circ, 160^\circ, 175^\circ, 180^\circ$).

b. Anisotropy

The anisotropic factor, ψ , is defined as

$$\psi(\theta, \phi, \theta_0) = \frac{\pi I(\theta, \phi, \theta_0)}{F_{\text{up}}(\theta_0)}, \quad (1)$$

where I is the radiance at a particular angle and F_{up} is the upward flux. ψ depends on the viewing angles θ and ϕ and the solar zenith angle θ_0 . The anisotropy is a measure of the departure from Lambertian behavior and would be identically one for a Lambertian reflector. A

mean value of anisotropy is computed from the 2D solution for each cloud sample, where I and F are the mean value of radiance and flux over the 10 km scene. If ψ were known exactly for a cloud field, a radiance measured at some given view angle could be used to accurately estimate the flux of energy from the whole hemisphere. Unfortunately, ψ is quite sensitive to cloud properties.

4. SINGULAR VALUE ANALYSIS

a. Theory

The mean anisotropy functions, ψ , for all the cloud samples are used as input to a Singular Value Decomposition (SVD) analysis to search for clusters of similar shapes. This analysis follows Ref. 5. Each discretized anisotropy function, $\psi(\theta_i, \phi_j, \theta_{0k})$, is written as a vector where the value of ψ at successive view angles (θ_i, ϕ_j) form the M components of the vector, Y_m . A deviation vector is then formed as: $dY_m = Y_m - \langle Y \rangle$, where $\langle Y \rangle$ is the mean vector formed by averaging all cloud sample. The N deviation vectors for all the cloud samples are then written as the columns of an $M \times N$ matrix. In this implementation, $M = 109$ and $N = 341$. Singular value decomposition, in this case following Ref. 6, is used to expand the matrix into three components:

$$dY = UDV^T, \quad (2)$$

where the central matrix, D , is a diagonal matrix whose elements d_1, d_2, \dots, d_L are the singular values. Note that L in general is not equal to either M or N .

Sorting the singular values into descending order allows the importance of each component to be assessed. The mean variance is given by:

$$\langle d^2 \rangle_{\text{random}} = \frac{1}{L} \sum_{k=1}^L d_k^2. \quad (3)$$

If we identify the value k' for which all variances before that are greater than the mean variance, then the first k' (largest) singular values can be identified as «degrees of freedom» for the problem; while the remaining values merely contribute noise.

The vectors in U are the orthogonal eigenmodes and can be used to categorize each anisotropic function as «closest» to a particular mode:

$$T = Y^T U, \quad (4)$$

T is a single row of numbers, and the largest number indicates the «cluster» to which the anisotropic function belongs.

The eigenmodes can also be used to approximately reconstruct each anisotropic function. One requires k' coefficients multiplying the eigenmodes identified in the degree of freedom analysis. These coefficients are simply the coefficients of U in Eq. (2), or $c = d_k V_k^T$.

b. Results

Results (Fig. 1) show that 4–6 mode shapes are generally sufficient to describe the anisotropic functions, for all solar zenith angles. Not only do these first 4–6 mode shapes have variance larger than the mean variance; but they cumulatively capture almost all the variance. This result suggests that there may be hope of describing the anisotropic variability of cloud fields with a relatively small number of parameters.

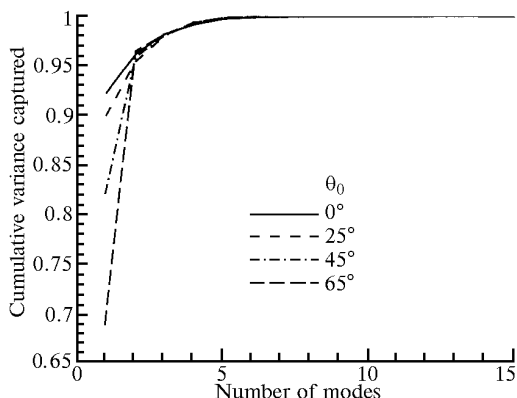


FIG. 1. Amount of anisotropic variance captured as a function of number of modes for several solar zenith angles.

Deviation mode shapes ($\psi_{\text{mode}} - \bar{\psi}$, where $\bar{\psi}$ is the overall mean anisotropic function) are given for overhead Sun in Fig. 2. Of particular interest is Mode 4, which is not entirely symmetric with respect to forward and backscattering in this case. This picks up on a few cloud samples in this dataset which contain oriented clouds and therefore have a preferred scattering direction even for overhead Sun.

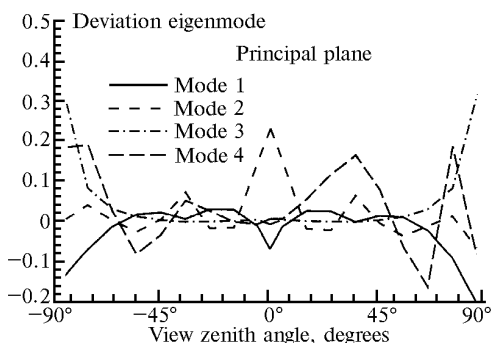


FIG. 2. First four deviation mode shapes in the principal plane for overhead Sun.

The coefficients of the first four mode shapes are shown in Fig. 3 for a solar zenith angle of 45° as a function of the cloud parameter to which each coefficient is most sensitive. The solid line in each figure is a least-squares fit to the points. The parameter σ_τ is the standard deviation of the cloud sample. ν is called the gamma function parameter, and

is defined as $\nu = (\bar{\tau}/\sigma)^2$ (Ref. 6). It is obvious that a single parameter fit is not sufficient to capture the complete variability of these coefficients. Furthermore, the parameter to which each coefficient is most sensitive changes at different solar zenith angles (see Table II).

TABLE II. Single parameter fit of SVD mode coefficients with best regression.

	$\theta_0 = 0^\circ$			$\theta_0 = 45^\circ$		
	Parameter	r^2	Std error	Parameter	r^2	Std error
C_1	A_c	0.84	11.5	A_c	0.77	8.39
C_2	$\text{Log}_{10}(\nu)$	0.34	6.71	σ_τ	0.31	4.17
C_3	$\text{Log}_{10}(\tau)$	0.29	11.5	$\text{Log}_{10}(\nu)$	0.45	13.1
C_4	σ_z	0.02	38.0	$\text{Log}_{10}(\tau)$	0.2	22.8

Table II summarizes the sensitivity of the first four mode coefficients, giving the parameter which results in the maximum linear regression coefficient, r^2 , and the resulting standard error in the fit. Note that, as suggested in Figure 3, the regression coefficient is not very large, especially for other than the first mode coefficient. Further, since using a different parameter (not shown) often results in a lower standard error, these single parameter fits cannot be assumed to provide a satisfactory representation of the variation of the mode coefficients. Here σ_z is the standard deviation of the cloud height, and is a measure of cloud bumpiness or shape. Other parameters which were considered, but which don't appear to capture the behavior of the coefficients, were a measure of cloud vertical to horizontal aspect ratio (AR) and the mean size of the gap between clouds ($\bar{\text{gap}}$). It may be that there exists a singular parameter which captures this variability better, but no such parameter has yet been found.

Because patterns do seem evident in the previous results, two-parameter linear regressions have also been performed for all combinations of the 7 cloud parameters considered above. Table III summarizes the combinations which result in the minimum standard error. Interestingly, the parameter providing the best single parameter fit is not always included in producing the best two parameter fit. Substantial reductions in standard error are found in most cases relative to the single parameter fits.

TABLE III. Two parameter fit of SVD mode coefficients with minimal error.

	$\theta_0 = 0^\circ$			$\theta_0 = 45^\circ$		
	Parameter		Std error	Parameter		Std error
	1	2		1	2	
C_1	A_c	σ_τ	3.52	σ_τ	$\bar{\text{gap}}$	3.99
C_2	$\text{Log}_{10}(\nu)$	σ_τ	6.02	σ_τ	AR	5.16
C_3	$\text{Log}_{10}(\tau)$	AR	4.47	AR	$\frac{\sigma_\tau}{\bar{\text{gap}}}$	6.95
C_4	$\text{Log}_{10}(\tau)$	AR	2.58	$\text{Log}_{10}(\nu)$	$\bar{\text{gap}}$	3.11

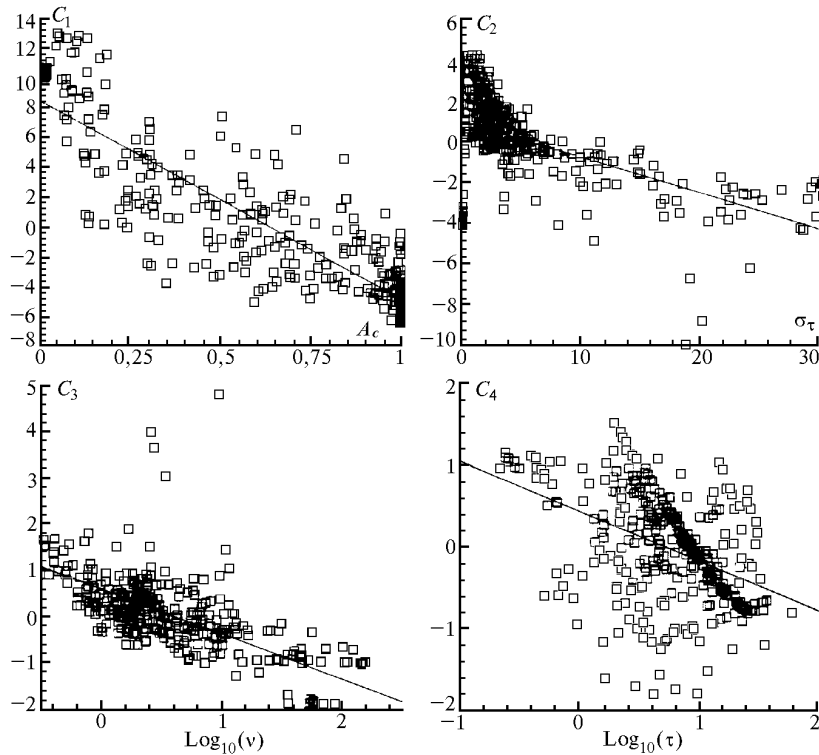


FIG. 3. Coefficients of first four mode shapes as a function of cloud parameter to which each is most sensitive, $\theta_0 = 45^\circ$.

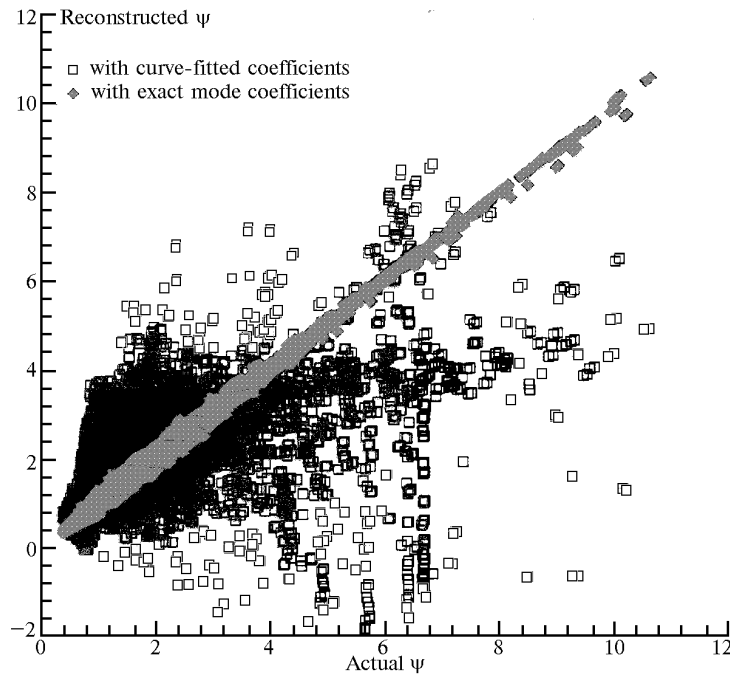


FIG. 4. Reconstructed versus original anisotropic function.

Figure 4 shows the reconstructed ψ plotted against the actual ψ . The solid gray symbols are for ψ reconstructed by combining the first 4 eigenmodes using the coefficients, c , obtained from the SVD analysis. The open symbols are for ψ reconstructed by combining the same four eigenmodes using coefficients obtained from the one or two parameter

linear curve fit as a function of a cloud property with minimum standard error. It is quite obvious that while the 4 SVD mode shapes provide an excellent reconstruction of the actual ψ function, the curve-fitted coefficients are inadequate. Factor of two differences are quite typical between the two reconstructions. The overall root-mean-square (RMS)

error is 40%. Even more troubling are the zero and negative values which are predicted by the curve-fitted reconstruction. Clearly such a reconstruction is not adequate for use in inverting radiance to flux.

c. Other evidence

A similar analysis (not shown) was previously performed on another set of theoretical results. In that case the cloud fields were much simpler. Constant effective radius of the cloud water droplets, constant extinction in each cloud column, and flat-topped clouds were assumed. In that case the reconstruction of the ψ function was somewhat better, following the high density area in Figure 4 without the outlying points – and certainly without zero and negative values of ψ . This suggests that the variability in cloud top shape, particle size, and extinction are likely candidates as controlling variables in reconstructing the eigenmode coefficients. However, the parameters that have so far been constructed in an attempt to capture this variability have clearly failed to reproduce the right shape.

The analysis was also repeated using only the overcast ($A_c > 0.99$) cloud scenes. In that case there is a much more systematic variation of the SVD coefficients with optical depth in particular. This results in a somewhat better reconstruction of ψ , with RMS errors on the order of 20% overall-half that in Fig. 4; but there are still a number of points near and below zero in the reconstruction.

5. CONCLUSIONS AND FUTURE DIRECTIONS

A theoretical analysis has been performed which suggests that it should be possible to capture the variability in the anisotropic behavior of clouds using 4–6

parameters. However, the results obtained to date using typical parameters such as cloud fraction and optical depth, as well as additional parameters describing the variability of optical depth and cloud shape, have not been found to produce the desired results. It is possible that a satisfactory fit of the coefficients could be obtained if the mode shapes could be transformed by linear combination into another orthogonal set; or if some new parameter which describes the variability of the cloud field could be identified. However, at this point there is no obvious strategy for how to do this.

ACKNOWLEDGMENTS

This work benefited greatly from conversations with Dr. G. Louis Smith, and Dr. Bruce R. Barkstrom, both of NASA Langley Research Center.

REFERENCES

1. Harshvardhan, B.A. Wielicki, and K.M. Ginger, *J. Climate* **7** (1987, 1994).
2. L.H. Chambers, B.A. Wielicki, and K.F. Evans, *J. Geophys. Res.* **102**, No. D2, 1779–1794 (1997).
3. N.G. Loeb, T. Varnai, and D.M. Winker, *J. Atmos. Sci.* **55**, 2960–2973 (1998).
4. K.F. Evans, *J. Atmos. Sci.* **55**, 249–446 (1998).
5. B.R. Barkstrom http://asd-www.larc.nasa.gov/cost_model/survey/gues_rslt.ps. 30–32 (1996).
6. C.L. Lawson and R.J. Hanson, *Solving Least Squares Problems* (Prentice-Hall, 1974).
7. H.W. Barker, B.A. Wielicki, and L. Parker, *J. Atmos. Sci.* **53**, No. 16, 2304–2316 (1996).